

Deconstructing Vibrational Motions on the Potential Energy Surfaces of Hydrogen-Bonded Complexes

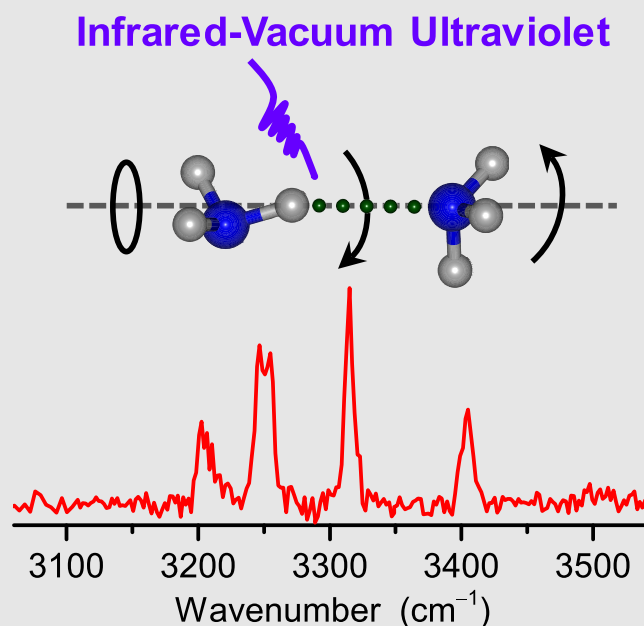
Bingbing Zhang^{1#}, Shuo Yang^{1,4#}, Qian-Rui Huang^{2#}, Shukang Jiang¹, Rongjun Chen^{1,4}, Xueming Yang^{1,3}, Dong H. Zhang¹, Zhaojun Zhang^{1*}, Jer-Lai Kuo^{2*} & Ling Jiang^{1*}

¹State Key Laboratory of Molecular Reaction Dynamics, Collaborative Innovation Center of Chemistry for Energy and Materials, Dalian Institute of Chemical Physics, Chinese Academy of Sciences, Dalian 116023, ²Institute of Atomic and Molecular Sciences, Academia Sinica, Taipei 10617, ³Department of Chemistry, School of Science, Southern University of Science and Technology, Shenzhen 518055, ⁴University of Chinese Academy of Sciences, Beijing 100049.

*Corresponding authors: zhangzhj@dicp.ac.cn; jlkuo@pub.iams.sinica.edu.tw; ljiang@dicp.ac.cn; #B. Zhang, S. Yang, and Q.-R. Huang contributed equally to this work.

Cite this: *CCS Chem.* **2020**, *2*, 829–835

Internal vibrations underlie transient structure formation, spectroscopy, and dynamics. However, at least two challenges exist when aiming to elucidate the contributions of vibrational motions on the potential energy surfaces. One is the acquisition of well-resolved experimental infrared spectra, and the other is the development of efficient theoretical methodologies that reliably predict band positions, relative intensities, and substructures. Here, we report size-specific infrared spectra of ammonia clusters to address these two challenges. Unprecedented agreement between experiment and state-of-the-art quantum simulations reveals that the vibrational spectra are mainly contributed by proton-donor ammonia. A striking Fermi resonance observed at approximately 3210 and 3250 cm^{-1} originates from the coupling of NH symmetric stretch fundamentals with overtones of free and hydrogen-bonded NH bending, respectively. These novel, intriguing findings contribute to a better understanding of vibrational motions in a large variety of hydrogen-bonded complexes with orders of magnitude improvements in spectral resolution, efficiency, and specificity.



Keywords: vibrational motion, potential energy surface, hydrogen bonding, Fermi resonance, ammonia cluster, infrared spectroscopy, quantum simulation, anharmonic algorithm calculation

Understanding the internal motions and intermolecular potentials that account for the structure, spectroscopy, and dynamics of flexible hydrogen-bonded and van der Waals complexes has been a great challenge for contemporary physical chemistry.^{1,2} Infrared (IR) spectroscopy can provide detailed information on vibrational motions on potential energy surfaces (PESs), which is an indispensable first step toward achieving quantitative understanding of the diverse phenomena associated with clusters, condensed matter, and biological systems at a microscopic level.^{1,3} However, direct comparison between theory and experiment for the band positions, relative intensities, and substructures of IR spectra of weakly bound molecular clusters is extremely difficult because the wave functions associated with the various bound states have significant amplitude at configurations far from the equilibrium geometry.^{1,3–5} It is becoming increasingly evident that the interpretation of experimental IR spectra of hydrogen-bonded clusters requires theoretical tools beyond the harmonic approximation.^{5–7}

Ammonia clusters are prototype systems for studying the interplay between different vibrational motions on flexible PESs.⁸ The hydrogen bond of the ammonia dimer is considerably bent from the ideal linear configuration (unlike that of the water dimer),⁹ which has led to extensive studies of this particular intermolecular interaction.^{8–19} It is now evident from both experimental and theoretical studies that the intermolecular PES of the ammonia dimer is indeed extremely flat.^{16–18} To disentangle the contributions of vibrational motions on the PES, one needs to achieve well-resolved vibrational spectra. IR spectra of ammonia dimers were measured previously,^{20,21} but the assignment of the structures and vibrational motions was not definitive due to the nominally low signal level and lack of high-level theoretical analysis. Here, we report the well-resolved IR spectra of size-selected ammonia dimers and trimers using an infrared–vacuum ultraviolet (IR–VUV) scheme. Clear spectral substructures observed in the very fluxional ammonia dimer are assigned by a comparison with high-level quantum simulations using a full-dimensional *ab initio* PES and the discrete variable representation (DVR) anharmonic algorithm. We thereby identify the global minimum energy structures and anharmonic coupling of different vibrational motions.

Experiments were performed using an IR–VUV apparatus (see the “Experimental Methods” section in the Supporting Information).²² Neutral ammonia clusters in a pulsed supersonic expansion beam were ionized by one-photon absorption of a VUV pulse and mass-analyzed in a reflectron time-of-flight mass spectrometer. IR spectra of the size-selected neutral cluster were recorded by monitoring the depletion in signal intensity for a specific cluster as a function of the IR wavelength.

Supporting Information Figure S1 shows the mass spectra of ammonia clusters generated by 118 nm single-photon ionization. Two series of ammonia clusters

ions are observed, one unprotonated $(\text{NH}_3)_n^+$ and the other protonated $\text{H}^+(\text{NH}_3)_n$. The 118 nm photoionization of neutral ammonia clusters creates the unprotonated $(\text{NH}_3)_n^+$ cations, which undergo very fast intracluster charge redistribution within 100 fs or less.^{23,24} The most thermodynamically and kinetically favorable reaction pathway is proton transfer and subsequent NH_2 loss.^{23–28} Previous experimental and theoretical studies have demonstrated that the protonated $\text{H}^+(\text{NH}_3)_n$ cluster ions are the main fragment arising from photoionized clusters due to intracluster ion–molecule reactions, and are the most prominent features in the mass spectrum.^{23–29} These characteristics explain why the protonated $\text{H}^+(\text{NH}_3)_n$ ions are so dominantly observed in the present mass spectra. The 118 nm single-photon ionization and dissociation mechanisms of ammonia cluster cations have been recently discussed.²⁸

The experimental IR spectra of size-selected $(\text{NH}_3)_2$ and $(\text{NH}_3)_3$ in the NH stretching region, monitored by ion signal intensities of the unprotonated $(\text{NH}_3)_2^+$ and $(\text{NH}_3)_3^+$ cations, are shown in Figures 1a and 1b, respectively. The IR spectra of $(\text{NH}_3)_2$ and $(\text{NH}_3)_3$ are different from each other, indicating that these IR spectra were measured with negligible contribution from larger clusters. Capital letters (A–D) are used for labeling experimental peaks. The present IR spectra comprise four main bands (labeled A–D), which are consistent with the previous IR–VUV studies (Supporting Information Figure S2).²⁰ For $(\text{NH}_3)_2$, a new substructure at 3223 cm^{-1} (labeled D′) is clearly resolved in the present measurement. In particular, when the IR laser power is lowered to 2 mJ/mm^2 , band D′ is still observed, but band D disappears (Supporting Information Figure S3), revealing a distinct dependence on the IR laser power. This indicates that different vibrational modes might be involved in bands D and D′. IR laser power dependence for infrared spectra of $(\text{NH}_3)_3$ is shown in Supporting Information Figure S4.

It is interesting to compare our results with previous measurements in helium droplets.²¹ The main features in the present spectra are consistent with those in the previous studies. The major discrepancy is the assignment of bands C and D that were presumed to originate from ammonia trimer or larger clusters. Scenarios rationalizing this contradiction include previous assignment of the bands to particular cluster sizes facilitated by measurements of the pressure dependence of the intensity, which may be not sensitive enough for size selection of ammonia clusters with weak binding energies. Our approach—the IR–VUV scheme of neutral $(\text{NH}_3)_2$ and $(\text{NH}_3)_3$, which monitors ion signal intensities of the unprotonated $(\text{NH}_3)_2^+$ and $(\text{NH}_3)_3^+$ cations—is free from spectral contamination due to the fact the IR-excited ammonia clusters dominantly dissociate into the protonated cluster cation mass channels in the 118 nm photoionization process.³⁰

To understand the hydrogen-bonding structures of these neutral ammonia clusters and their IR spectra,

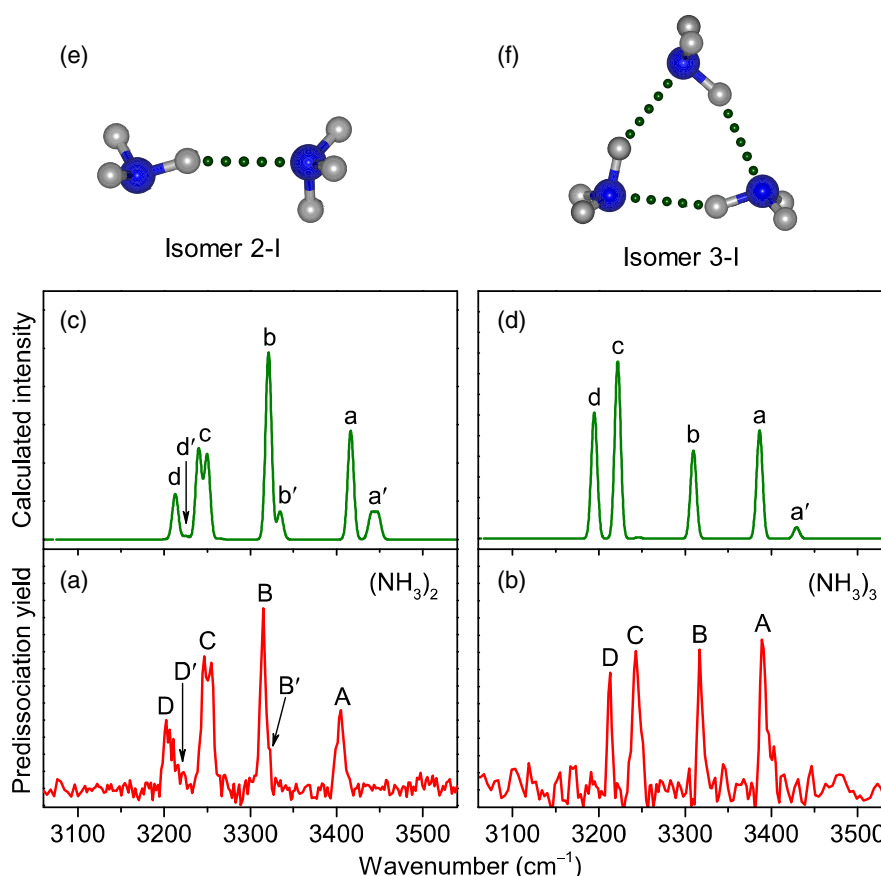


Figure 1 | Experimental IR spectra of $(\text{NH}_3)_2$ (a) and $(\text{NH}_3)_3$ (b). Simulated spectrum of isomer 2-I for $(\text{NH}_3)_2$ calculated using a full-dimensional *ab initio* PES at the CCSD(T)-F12/aug-cc-pVTZ level coupled with 10 high-frequency vibrational modes (c) and that of isomer 3-I for $(\text{NH}_3)_3$ obtained from DVR anharmonic calculations at the CCSD(T)-F12/aug-cc-pVTZ level coupled with five high-frequency vibrational modes (d). The corresponding dimer and trimer structures are shown (e and f).

quantum chemical calculations were carried out with wave function theory at the CCSD/aug-cc-pVDZ (AVDZ) level to predict the harmonic vibrational spectra (see Supporting Information for computational details). The optimized structures for neutral ammonia clusters are shown in Supporting Information Figure S5. The global minimum structure of the ammonia dimer is found to be an eclipsed structure with C_s symmetry (labeled 2-I). The 2-II and 2-III structures appear to be transition states¹⁶ that have the imaginary vibrational frequencies of $45i$ and $94i$ cm^{-1} , respectively. The ammonia trimer has a cyclic structure (labeled 3-I) with slightly shorter hydrogen bonds than the ammonia dimer. These results are in accord with previous studies.^{12,13,15,16,19} The CCSD/AVDZ calculated harmonic vibrational spectra of the ammonia dimer and trimer are shown in Supporting Information Figures S6 and S7, respectively. Lower case letters (a-d) are used for the labeling of theoretical peaks.

For the 2-I, 2-II, and 2-III isomers (Supporting Information Figure S6), the CCSD/AVDZ calculated harmonic vibrational spectra yield only two main bands,

leaving the C and D bands unassigned. The antisymmetric stretch of a hydrogen-bonded NH in proton-donor ammonia is predicted to be approximately 3410 cm^{-1} (band a), which is close to the experimental value of band A (3407 cm^{-1}); the calculated symmetric stretch frequency of NH in proton-donor ammonia of band b (3283 cm^{-1}) is much lower than the experimental value of band B (3315 cm^{-1}). Similar results have also been found for the ammonia trimer (Supporting Information Figure S7). It is clear that the experimental spectra cannot be reproduced by rescaling the harmonic model. A highly accurate description of hydrogen-bonding potentials is thus needed in order to calculate the band positions and intensities for direct comparison with experiments.

The clear spectral substructures displayed by $(\text{NH}_3)_2$ provide detailed structural and dynamical information at the fingerprint level. The ammonia dimer is small enough to be accurately treated with high-level electronic structure theory. For unequivocal assignments of the experimental spectra, a full-dimensional *ab initio* PES at the CCSD(T)-F12/aug-cc-pVTZ (AVTZ) level was

Table 1 | Experimental Band Positions (cm^{-1}) for $(\text{NH}_3)_2$, Vibrational Frequencies (cm^{-1}) Calculated from a Full-Dimensional PES of Isomer 2-I, and Band Assignments

Label	Exp.	Theory	Assignment
A	3407	3416	Antisymmetric stretch of hydrogen-bonded NH in proton-donor ammonia ($\nu_{3\text{HB}}^{\text{D}}$)
B'	3323	3334	Symmetric stretch of NH in proton-acceptor ammonia (ν_1^{A})
B	3315	3321	Symmetric stretch of NH in proton-donor ammonia (ν_1^{D})
C	3251	3240	Fermi resonance of NH symmetric stretch (ν_1^{D}) with bend overtone ($2\nu_{4\text{HB}}^{\text{D}}$) and bend combination ($\nu_{4\text{free}}^{\text{D}} + \nu_4^{\text{A}}$)
	3259	3250	
D'	3223	3225	Bend overtone ($2\nu_{4,1}^{\text{A}}$)
D	3207	3213	Fermi resonance between NH symmetric stretch (ν_1^{D}) and bend overtones ($2\nu_{4\text{free}}^{\text{D}}$)

constructed for the ammonia dimer using the fundamental invariant neural network (FI-NN) fitting method (see [Supporting Information](#) for details).³¹ In the calculations of anharmonic vibrational spectra, 10 high-frequency intramolecular vibrational modes (that contain all the stretching and bending modes of both the proton-donor and proton-acceptor ammonia, [Supporting Information Table S2](#)) were included in potential-optimized discrete variable representation (PODVR) grid points.³² The calculated anharmonic vibrational spectrum of isomer 2-I is shown in Figure 1c, and those of isomers 2-II and 2-III are given in [Supporting Information Figure S8](#).

Overall, good agreement between the experimental and simulated anharmonic vibrational spectra of 2-I indicates that the 2-I structure is the main isomer present in the experiment. For isomers 2-II and 2-III, the calculated patterns of bands c and d are discrepant from the experimental spectra ([Supporting Information Figure S8](#)). In the full-dimensional PES calculated vibrational spectrum of isomer 2-I (Figure 1c), the 3416 cm^{-1} band (labeled a) is due to the antisymmetric stretch of hydrogen-bonded NH in proton-donor ammonia ($\nu_{3\text{HB}}^{\text{D}}$), which is consistent with the experimental value of band A (3407 cm^{-1}) (Table 1). The calculated band b at 3321 cm^{-1} is attributed to the symmetric stretch of NH in proton-donor ammonia (ν_1^{D}), which agrees with the experimental value of band B (3315 cm^{-1}). The calculated band b' (3334 cm^{-1}) is resolved as a shoulder of band B in the experimental spectrum (band B', 3323 cm^{-1}), which is ascribed to the symmetric stretch of NH in proton-acceptor ammonia (ν_1^{A}). The calculated bands at 3240 and 3250 cm^{-1} (band c) are assigned to a Fermi resonance between the NH symmetric stretch (ν_1^{D}) and bend overtone ($2\nu_{4\text{HB}}^{\text{D}}$) and agree well with the experimental values of band C (3251 and 3259 cm^{-1}). The calculated band d (3213 cm^{-1}) is assigned to a Fermi resonance between the NH symmetric stretch (ν_1^{D}) and bend overtones ($2\nu_{4\text{free}}^{\text{D}}$), which reproduces the experimental band D (3207 cm^{-1}). The bend overtone of $2\nu_{4,1}^{\text{A}}$ is found to be responsible for band d', which is interpreted as corresponding to the experimental band D'. Band a' (3445 cm^{-1}) mainly results from the antisymmetric stretch of free NH in proton-donor

ammonia ($\nu_{3\text{free}}^{\text{D}}$) and antisymmetric stretches of NH in proton-acceptor ammonia (ν_3^{A} and $\nu_{3,1}^{\text{A}}$) and is not observed experimentally.

To understand the contribution of vibrational motions to the vibrational spectra, five-, six-, and seven-mode quantum simulations based on the full-dimensional ab initio PESs at the CCSD(T)-F12/AVTZ level were also carried out for isomer 2-I. The calculated spectra are compared in Figure 2. It can be seen from Figures 2a and 2b that if the symmetric stretch of NH in proton-donor ammonia (ν_1^{D}) is excluded, the band positions of bands a-d are remarkably blue-shifted from the experimental values; the intensities of bands b-d are substantially smaller than that of band a; the a' band does not appear, indicating that the ν_1^{D} mode plays a significant role in the coupling in the PES. The bend of NH in hydrogen-acceptor ammonia (ν_4^{A}) makes a negligible contribution to the calculated bands (Figure 2c). When the symmetric stretch of NH in hydrogen-acceptor ammonia (ν_1^{A}) and antisymmetric stretches of NH in hydrogen-acceptor ammonia (ν_3^{A} and $\nu_{3,1}^{\text{A}}$) are simultaneously added, the splitting of band c and substructures of bands b' and d' appear (Figure 2d).

To analyze the coupling between normal modes in proton-donor and proton-acceptor ammonia, we used localized normal modes to expand the vibrational wave function via the DVR anharmonic method.³³ The vibrational spectrum calculated using all five modes localized on the proton-donor ammonia of isomer 2-I ([Supporting Information Table S3](#)) is shown in Figure 3a. The minor peak at 3431 cm^{-1} (band a') is assigned as $\nu_{3\text{free}}^{\text{D}}$, and the more intense peak at 3402 cm^{-1} (band a) is assigned as $\nu_{3\text{HB}}^{\text{D}}$. The next three peaks, at 3321 , 3241 , and 3206 cm^{-1} (bands b, c, and d, respectively), result from a Fermi resonance between NH symmetric stretching (ν_1^{D}) and bending overtones ($2\nu_{4\text{free}}^{\text{D}}$ and $2\nu_{4\text{HB}}^{\text{D}}$). The intensities of these three peaks mainly come from the ν_1^{D} mode. This Fermi resonance coupling has been discussed previously using anharmonic calculations based on a quartic potential evaluated at the MP2/AVDZ level,¹⁹ but higher-level calculations at the CCSD(T)-F12/AVTZ level yield much improved agreements.

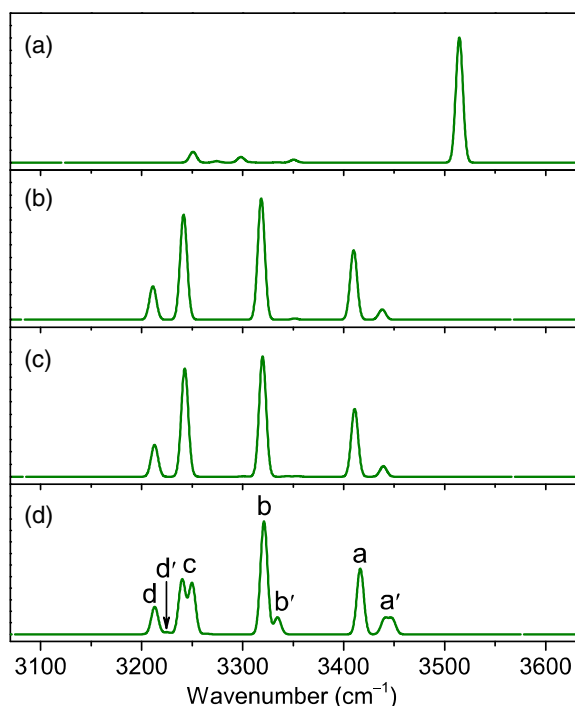


Figure 2 | Comparison of different multiple-mode calculated spectra of isomer 2-I for $(\text{NH}_3)_2$ based on the full-dimensional *ab initio* PES at the CCSD(T)-F12/AVTZ level. (a) Five modes: $\nu_{4\text{free}}^D$, $\nu_{4\text{HB}}^D$, $\nu_{3\text{HB}}^D$, $\nu_{3\text{free}}^D$, and $\nu_{4'}^A$. (b) Six modes: $\nu_{4\text{free}}^D$, $\nu_{4\text{HB}}^D$, $\nu_{3\text{HB}}^D$, $\nu_{3\text{free}}^D$, ν_1^D , and $\nu_{4'}^A$. (c) Seven modes: $\nu_{4\text{free}}^D$, $\nu_{4\text{HB}}^D$, $\nu_{3\text{HB}}^D$, $\nu_{3\text{free}}^D$, ν_1^D , $\nu_{4''}^A$, and $\nu_{4'}^A$. (d) 10 modes: $\nu_{4\text{free}}^D$, $\nu_{4\text{HB}}^D$, $\nu_{3\text{HB}}^D$, $\nu_{3\text{free}}^D$, ν_1^D , $\nu_{4''}^A$, $\nu_{4'}^A$, ν_1^A , ν_3^A , and $\nu_{3'}^A$.

The vibrational spectrum calculated using all five modes localized on the proton-acceptor ammonia of isomer 2-I is shown in Figure 3b. The normal modes of proton-acceptor ammonia resemble those of ammonia not donating a proton and the overall intensities of vibrational motions in the IR spectrum of proton-acceptor ammonia are weaker than those of proton-donor ammonia. The band at 3431 cm^{-1} contains the two antisymmetric stretches of NH in the proton-acceptor ammonia (ν_3^A and ν_3^A). The ν_1^A mode appears at 3332 cm^{-1} . The two bend overtone transitions of ν_4^A and ν_4^A , that couple to the ν_3 modes appear at 3223 cm^{-1} .

The vibrational spectrum calculated using the aforementioned 10 modes in both proton-donor and proton-acceptor ammonia of isomer 2-I is shown in Figure 3c. Its overall shape is close to the sum of the spectra of the donor and the acceptor. This similarity is direct evidence that the vibrational coupling between the normal modes in donor/acceptor ammonia is not strong. The most noticeable difference is the splitting of band c, which is consistent with that of experimental band C (Figure 1a). Our analysis indicates that this splitting is a result of the coupling of ν_1^D with a bend overtone ($2\nu_{4\text{HB}}^D$)

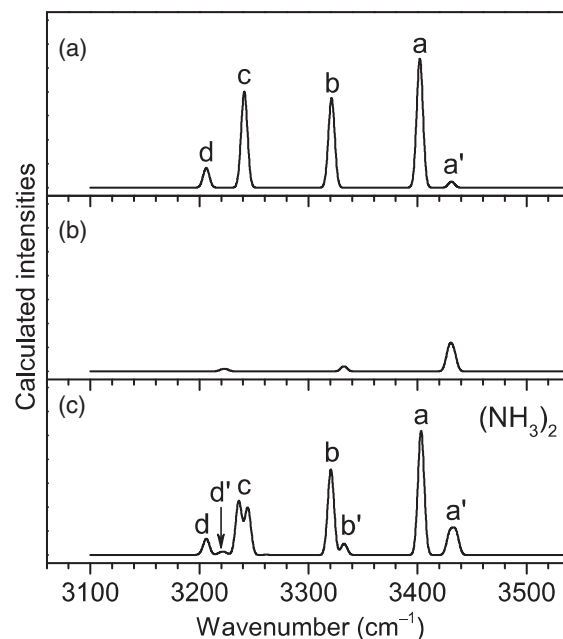


Figure 3 | Simulated vibrational spectra of isomer 2-I obtained from DVR anharmonic calculations at the CCSD(T)-F12/AVTZ level including five high-frequency vibrational modes of proton-donor ammonia (a), five high-frequency vibrational modes of proton-acceptor ammonia (b), and 10 high-frequency vibrational modes of both proton-donor and proton-acceptor ammonia (c).

and the bend combination of one quanta of $\nu_{4\text{free}}^D$ and one quanta of ν_4^A . The splitting of band c is reproduced by the 10-mode anharmonic calculation but not by two individual 5-mode calculations.

The 10-mode DVR anharmonic calculation (Figure 3c) yields essentially the same vibrational spectrum as the full-dimensional PES calculation (Figure 1c). Thus, the assignment of the experimental spectrum of the ammonia dimer is straightforward based on the earlier analysis, which is given in Table 1. The a' band in the simulated spectra is not seen clearly in the experimental spectrum. The absence of band a' is probably because the dipole derivative of $\nu_{3\text{free}}$ is perpendicular to the molecular axis; in this case of K-type rotational features, this leads to a relatively more dispersed rotational profile. By comparison, the $\nu_{3\text{HB}}$ has a parallel-type rotational contour that resembles a band slightly broader than usual. A similar situation has been observed in the vibrational spectra of symmetric and antisymmetric free OH modes of $\text{H}_3\text{O}^+\cdots\text{N}_2$ and $\text{H}_3\text{O}^+\cdots\text{Ar}$.³⁴ To support our arguments, we simulated the rotational profiles of $\nu_{3\text{free}}$ and $\nu_{3\text{HB}}$ using PGOPHER³⁵ at different rotational temperatures. The resulting spectra are shown in Supporting Information Figure S9. In the simulated rovibrational spectra of the ammonia dimer, $\nu_{3\text{free}}$ (band a') is remarkably smeared out, consistent with its absence from the experimental spectrum.

FI-NN was not applied to the ammonia trimer, because it is still beyond the capacity of current FI-NN technique to construct a global PES for $(\text{NH}_3)_3$ (with 30 degrees of freedom) with spectroscopic accuracy. The vibrational spectrum of the ammonia trimer was calculated using DVR anharmonic calculations at the CCSD(T)-F12/aug-cc-pVTZ level coupled with all five modes localized on one ammonia molecule, which is shown in Figure 1d. The vibrational coupling in the ammonia trimer is very similar to that in the proton-donor ammonia of the ammonia dimer. Band a' of the ammonia trimer is assigned to $\nu_{3\text{free}}^{\text{D}}$, band a is assigned to $\nu_{4\text{HB}}^{\text{D}}$, and bands b, c, and d are a consequence of a Fermi resonance of ν_1^{D} and bend overtones of $\nu_{4\text{HB}}^{\text{D}}/\nu_{4\text{free}}^{\text{D}}$ (Supporting Information Table S1). The relative intensities of experimental bands C and D are stronger in the ammonia trimer than in the ammonia dimer. This difference is due to the stronger hydrogen bond in $(\text{NH}_3)_3$ than in $(\text{NH}_3)_2$. Thus, the frequency of ν_1^{D} in $(\text{NH}_3)_3$ is red-shifted compared with that in $(\text{NH}_3)_2$. Such features in the experimental IR spectra of $(\text{NH}_3)_2$ and $(\text{NH}_3)_3$ are faithfully captured by our ab initio anharmonic calculations (Figure 1).

In summary, vibrational spectra of ammonia clusters were investigated using an IR-VUV technique and high-level quantum simulations. Direct comparison between theory and experiment for the band positions, relative intensities, and substructures of IR spectra has been successfully achieved. Our analysis reveals that proton-donor ammonia is mainly responsible for the vibrational spectra. The significant Fermi resonance observed in the spectra is principally ascribed to the coupling between NH symmetric stretch fundamentals and bend overtones of the proton-donor ammonia. These results have important implications for studying the role of internal motions and intermolecular potentials in the transient structure formation, spectroscopy, and dynamics of hydrogen-bonded complexes in, for example, atmospheric, biological, and astrophysical environments.

Methods

Experimental and Theoretical Methods are available in Supporting Information.

Supporting Information

Supporting Information is available.

Conflicts of Interest

There are no conflicts to declare.

Acknowledgments

This work was supported by the National Natural Science Foundation of China (grant nos. 21673231 and 21688102),

the Strategic Priority Research Program of the Chinese Academy of Sciences (CAS) (grant no. XDB17000000), the Dalian Institute of Chemical Physics (DICP DCLS201702), and K.C. Wong Education Foundation (GJTD-2018-06). Q.-R.H. and J.-L.K. were supported by the Ministry of Science and Technology of Taiwan (MOST-106-2811-M-001-051 and MOST-107-2628-M-001-002-MY4) and the Academia Sinica.

References

1. Muller-Dethlefs, K.; Hobza, P. Noncovalent Interactions: A Challenge for Experiment and Theory. *Chem. Rev.* **2000**, *100*, 143–167.
2. Lee, J.; Crampton, K. T.; Tallarida, N.; Apkarian, V. A. Visualizing Vibrational Normal Modes of A Single Molecule with Atomically Confined Light. *Nature* **2019**, *568*, 78–82.
3. Wormer, P. E. S.; van der Avoird, A. Intermolecular Potentials, Internal Motions, and Spectra of van der Waals and Hydrogen-Bonded Complexes. *Chem. Rev.* **2000**, *100*, 4109–4143.
4. Bacic, Z.; Miller, R. E. Molecular Clusters: Structure and Dynamics of Weakly Bound Systems. *J. Phys. Chem.* **1996**, *100*, 12945–12959.
5. Qu, C.; Bowman, J. M. Quantum Approaches to Vibrational Dynamics and Spectroscopy: Is Ease of Interpretation Sacrificed as Rigor Increases? *Phys. Chem. Chem. Phys.* **2019**, *21*, 3397–3413.
6. Asmis, K. R.; Pivonka, N. L.; Santambrogio, G.; Brummer, M.; Kaposta, C.; Neumark, D. M.; Woste, L. Gas-Phase Infrared Spectrum of the Protonated Water Dimer. *Science* **2003**, *299*, 1375–1377.
7. Baer, M.; Marx, D.; Mathias, G. Theoretical Messenger Spectroscopy of Microsolvated Hydronium and Zundel Cations. *Angew. Chem., Int. Ed.* **2010**, *49*, 7346–7349.
8. Nelson, D. D.; Fraser, G. T.; Klemperer, W. Does Ammonia Hydrogen Bond? *Science* **1987**, *238*, 1670–1674.
9. Nelson, D. D.; Fraser, G. T.; Klemperer, W. Ammonia Dimer: A Surprising Structure. *J. Chem. Phys.* **1985**, *83*, 6201–6208.
10. Olthof, E. H. T.; Vanderavoud, A.; Wormer, P. E. S. Structure, Internal Mobility, and Spectrum of the Ammonia Dimer: Calculation of the Vibration-Rotation-Tunneling States. *J. Chem. Phys.* **1994**, *101*, 8430–8442.
11. Olthof, E. H. T.; Vanderavoud, A.; Wormer, P. E. S.; Loeser, J. G.; Saykally, R. J. The Nature of Monomer Inversion in the Ammonia Dimer. *J. Chem. Phys.* **1994**, *101*, 8443–8454.
12. Lee, J. S.; Park, S. Y. Ab Initio Study of $(\text{NH}_3)_2$: Accurate Structure and Energetics. *J. Chem. Phys.* **2000**, *112*, 230–237.
13. Beu, T. A.; Buck, U. Structure of Ammonia Clusters from $n = 3$ to 18. *J. Chem. Phys.* **2001**, *114*, 7848–7852.
14. Beu, T. A.; Buck, U. Vibrational Spectra of Ammonia Clusters from $n = 3$ to 18. *J. Chem. Phys.* **2001**, *114*, 7853–7858.
15. Kulkarni, S. A.; Pathak, R. K. Ab Initio Investigations on Neutral Clusters of Ammonia: $(\text{NH}_3)_n$ ($n = 2-6$). *Chem. Phys. Lett.* **2001**, *336*, 278–283.

16. Boese, A. D.; Chandra, A.; Martin, J. M. L.; Marx, D. From Ab Initio Quantum Chemistry to Molecular Dynamics: The Delicate Case of Hydrogen Bonding in Ammonia. *J. Chem. Phys.* **2003**, *119*, 5965–5980.
17. Lin, W.; Han, J.-X.; Takahashi, L. K.; Loeser, J. G.; Saykally, R. J. Terahertz Vibration-Rotation-Tunneling Spectroscopy of the Ammonia Dimer: Characterization of an Out of Plane Vibration. *J. Phys. Chem. A* **2006**, *110*, 8011–8016.
18. Lin, W.; Han, J.-X.; Takahashi, L. K.; Loeser, J. G.; Saykally, R. J. Terahertz Vibration-Rotation-Tunneling Spectroscopy of the Ammonia Dimer. II. A-E States of an Out-of-Plane Vibration and an In-Plane Vibration. *J. Phys. Chem. A* **2007**, *111*, 9680–9687.
19. Ho, K.-L.; Lee, L.-Y.; Katada, M.; Fujii, A.; Kuo, J.-L. An Ab Initio Anharmonic Approach to Study Vibrational Spectra of Small Ammonia Clusters. *Phys. Chem. Chem. Phys.* **2016**, *18*, 30498–30506.
20. Matsuda, Y.; Mori, M.; Hachiya, M.; Fujii, A.; Mikami, N. Infrared Spectroscopy of Size-Selected Neutral Clusters Combined with Vacuum-Ultraviolet-Photoionization Mass Spectrometry. *Chem. Phys. Lett.* **2006**, *422*, 378–381.
21. Slipchenko, M. N.; Sartakov, B. G.; Vilesov, A. F.; Xantheas, S. S. Study of NH Stretching Vibrations in Small Ammonia Clusters by Infrared Spectroscopy in He Droplets and Ab Initio Calculations. *J. Phys. Chem. A* **2007**, *111*, 7460–7471.
22. Zhang, B.; Yu, Y.; Zhang, Z.; Zhang, Y.; Jiang, S.; Li, Q.; Yang, S.; Hu, H.; Zhang, W.; Dai, D.; Wu, G. Infrared Spectroscopy of Neutral Water Dimer Based on a Tunable Vacuum Ultraviolet Free Electron Laser. *J. Phys. Chem. Lett.* **2020**, *11*, 851–855.
23. Purnell, J.; Wei, S.; Buzzza, S. A.; Castleman, A. W. Formation and Protonated Ammonia Clusters Probed by a Femtosecond Laser. *J. Phys. Chem.* **1993**, *97*, 12530–12534.
24. Buzzza, S. A.; Wei, S.; Purnell, J.; Castleman, A. W. Formation and Metastable Decomposition of Unprotonated Ammonia Cluster Ions upon Femtosecond Ionization. *J. Chem. Phys.* **1995**, *102*, 4832–4841.
25. Shinohara, H.; Nishi, N.; Washida, N. Photoionization of Ammonia Clusters in a Pulsed Supersonic Nozzle Beam by Vacuum-UV Rare-Gas Resonance Lines. *Chem. Phys. Lett.* **1984**, *106*, 302–306.
26. Shinohara, H.; Nishi, N.; Washida, N. Photoionization of Ammonia Clusters: Detection and Distribution of Unprotonated Cluster Ions $(\text{NH}_3)_n^+$, $n = 2$ –25. *J. Chem. Phys.* **1985**, *83*, 1939–1947.
27. Peifer, W. R.; Coolbaugh, M. T.; Garvey, J. F. Observation of “Magic Numbers” in the Population Distributions of the $(\text{NH}_3)_{n-1}\text{NH}_2^+$ and $(\text{NH}_3)_{n-1}\text{H}_2^+$ Cluster Ions: Implications for Cluster Ion Structures. *J. Chem. Phys.* **1989**, *91*, 6684–6690.
28. Yuan, B.; Shin, J.-W.; Bernstein, E. R. Dynamics and Fragmentation of van der Waals and Hydrogen Bonded Cluster Cations: $(\text{NH}_3)_n$ and $(\text{NH}_3\text{BH}_3)_n$ Ionized at 10.51 eV. *J. Chem. Phys.* **2016**, *144*, 144315.
29. Park, J. K. Ab Initio Studies for Geometrical Structures of Ammonia Cluster Cations. *J. Phys. Chem. A* **2000**, *104*, 5093–5100.
30. Matsuda, Y.; Mikami, N.; Fujii, A. Vibrational Spectroscopy of Size-Selected Neutral and Cationic Clusters Combined with Vacuum-Ultraviolet One-Photon Ionization Detection. *Phys. Chem. Chem. Phys.* **2009**, *11*, 1279–1290.
31. Shao, K.; Chen, J.; Zhao, Z.; Zhang, D. H. Fitting Potential Energy Surfaces with Fundamental Invariant Neural Network. *J. Chem. Phys.* **2016**, *145*, 071101.
32. Zhao, Z.; Chen, J.; Zhang, Z.; Zhang, D. H.; Lauvergnat, D.; Gatti, F. Full-Dimensional Vibrational Calculations of Five-Atom Molecules using a Combination of Radau and Jacobi Coordinates: Applications to Methane and Fluoromethane. *J. Chem. Phys.* **2016**, *144*, 204302.
33. Zhang, B.; Huang, Q. R.; Jiang, S.; Chen, L. W.; Hsu, P. J.; Wang, C.; Hao, C.; Kong, X.; Dai, D.; Yang, X.; Kuo, J. L., Infrared Spectra of Neutral Dimethylamine Clusters: An Infrared-Vacuum Ultraviolet Spectroscopic and Anharmonic Vibrational Calculation Study. *J. Chem. Phys.* **2019**, *150*, 064317.
34. Huang, Q.-R.; Nishigori, T.; Katada, M.; Fujii, A.; Kuo, J.-L. Fermi Resonance in Solvated H^3O^+ : A Counter-Intuitive Trend Confirmed via a Joint Experimental and Theoretical Investigation. *Phys. Chem. Chem. Phys.* **2018**, *20*, 13836–13844.
35. Western, C. M. PGOPHER: A Program for Simulating Rotational, Vibrational and Electronic Spectra. *J. Quant. Spectrosc. Radiat. Transfer.* **2017**, *186*, 221–242.